Postprint of: Sobaszek M., Strąkowski M., Skowroński Ł., Siuzdak K., Sawczak M., Własny I., Wysmołek A., Wieloszyńska A., Pluciński J., Bogdanowicz R., In-situ monitoring of electropolymerization processes at boron-doped diamond electrodes by Mach-Zehnder interferometer, Sensors and Actuators B: Chemical, Vol. 304 (2020), 127315, DOI: 10.1016/j.snb.2019.127315

In-situ monitoring of electropolymerization processes at boron-doped diamond electrodes by Mach-Zehnder interferometer

Michał Sobaszek[1*], Marcin Strąkowski[1], Łukasz Skowroński[3], Katarzyna Siuzdak[4], Mirosław Sawczak[4], Igor Własny[5], Andrzej Wysmołek[5], Aleksandra Wieloszyńska[1], Jerzy Pluciński[1] and Robert Bogdanowicz[1]

[1] Department of Metrology and Optoelectronics, Faculty of Electronics, Telecommunications and Informatics, Gdansk University of Technology, G. Narutowicza St. 11/12, 80-233 Gdansk, Poland

[3]Institute of Mathematics and Physics, University of Technology and Life Sciences, Kaliskiego St. 7, 85-789 Bydgoszcz, Poland

[4]Centre for Plasma and Laser Engineering, The Szewalski Institute of Fluid-Flow Machinery, Polish Academy of Sciences, Fiszera St. 14, 80-231 Gdansk, Poland

[5]Faculty of Physics, University of Warsaw, Pasteura St. 5, 02-093 Warsaw, Poland

***Corresponding author: e-mail: micsobas@pg.edu.pl (Michał Sobaszek); Tel.: +48-58-347-15-03; Fax: +48 58-347-18-48**

Abstract

In this work, the Mach-Zehnder interferometer was designed to monitor the electrochemical processes conducted at boron-doped diamond electrode surface. The diamond electrodes were synthesized via Microwave Plasma-Assisted Chemical Vapor Deposition on optical grade quartz glass. The achieved transmittance in working are of diamond electrodes reached 55%. A cage system-based Mach-Zehnder interferometer was used which allowed the insertion of thin-layer electrochemical cells. Electrochemical studies were carried out in a thin-layer working cell. The application of such setup, allows to combine optical monitoring of surface of the working electrode during electrochemical measurements, electropolymerization or surface modification. The conducted investigation shows that during surface modification by melamine the phase shift is up to 0.0328 μm^{-1}. The aforementioned set up can be applied for in situ monitoring of surface modifications with various compounds, and to detect organic substances whose oxidation or reduction products absorb onto the electrode surface.

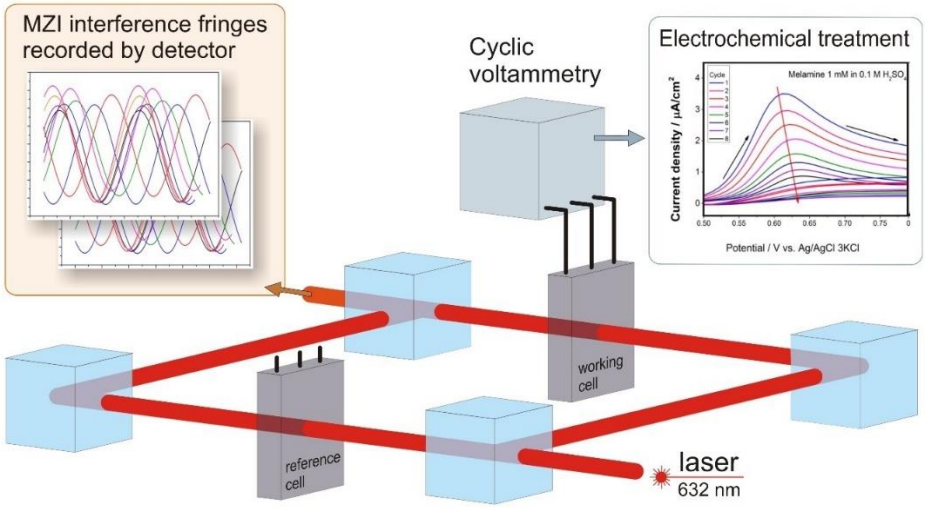

Keywords

Boron-doped diamond; in-situ monitoring; Mach-Zehnder interferometer; cyclic voltammetry; spectroelectrochemistry; melamine

1. Introduction

Nowadays, the development and fabrication of electrochemical sensors require the modification of electrode's surface with the reactive molecules [1–4]. The lack of chemically reactive groups precludes the attachment of organic compounds to the surface. Despite the outstanding electrochemical properties of boron-doped diamond (BDD) such as a wide working-potential window, low background current, and inherent biocompatibility, the BDD electrodes require the surface modification. Thus, many efforts are undertaken in the scope of the BDD electrodes' surface modification in order to improve the biosensing performance by chemically functional groups for the covalent coupling of important organic compounds [5]. The BDD electrodes can be modified by various techniques, namely, chemical [6], plasmo-chemical [7], photochemical [8] or electrochemical [9] methods. Moreover, the modification of electrodes is not always intended, e.g. many organic compounds form a polymeric film on the electrode's surface during the electrochemical detection [10,11]. Such modification can be an object of measurement. In order to monitor the modification of electrodes, ex situ techniques such as XPS, FTIR [12], wettability [13] or spectroscopic ellipsometry are used. However, the use the aforementioned techniques may be time-consuming or costly. Thus, there is a constant need for developing sensitive tools which would enable in situ monitoring of electrochemically-induced surface modifications. Among the very useful techniques that allow for optical monitoring during the electrochemical processes is spectroelectrochemistry. However, this method requires highly optically transparent electrodes [14,15]. The most attractive electrode for the above setup would be optically transparent boron-doped diamond electrode. In the case of polycrystalline diamond, the optical transparency depends on its chemical composition, doping level, thickness, and the grain size [16]–[19]. Boron-doped diamond electrodes are transparent within the visible range (300-900 nm) and far-IR. Furthermore, the optical properties of diamond can be optimized by changing the deposition conditions [16–19].

The diamond optically transparent electrode (OTE) possesses key advantages in comparison to the indium-doped tin oxide (ITO) electrode on quartz. It delivers reproducible responsiveness and stability in harsh chemical environments. On the other hand, ITO provides high conductivity and high optical transparency, but according to the literature, it is unstable in strongly acidic and alkaline media and in chlorinated organic solvents [15].

Spectroelectrochemistry is a powerful tool which includes typical methods such as absorption spectroscopy in the ultraviolet, visible, near-infrared, and infrared regions used for electrochemical measurements [20]. The other method types are Raman scattering spectroscopy and magnetic resonance-based techniques [21,22]. Typically, the spectroscopic response is monitored in situ for the electrochemical reactions carried out under controlled conditions. The main problem is to correlate the obtained results, which concerns the concentrations that have to be higher for some of spectroelectrochemical measurements due to the insufficient band intensity. While the desire for adequate spectroscopic response may thus require higher concentrations of up to 0.05 mol dm^{-3}, the comparison with typical CV measurements at 0.001 mol dm^{-3} analyte concentration can lead to inconsistencies, especially for processes involving chemical reactions. Another encountered problem relates to monitoring the modifications on the electrode's surface. There are many organic compounds undergoing electro-polymerization during the detection step, which results in the electrode poisoning.

Therefore, in this paper we present a novel approach to spectroelectrochemistry that is based on replacing the absorbance measurements with the interferometric measurements. The measurement of phase change allows the determination of change in optical path, which results in the change in refractive index. We chose Mach-Zehnder interferometer (MZI) as a measuring equipment because it is a dual beam interferometer that enables precise measurements of refractive index, with a sensitivity of up to 1.8 10^{-6} refractive index units (RIU) [23]. MZI was also successfully used by other research groups to construct the refractive index sensors [24–26]. The thin boron-doped nanocrystalline diamond (B-NCD) film was deposited by Microwave Plasma-Assisted Chemical Vapor Deposition (MWPACVD) process on optical grade quartz glass. For this study, we chose 5000 ppm boron doping electrode due to the best compromise between optical and electrical parameters [19,27]. Scanning Electron Microscope was used to determine surface morphology of B-NCD electrodes. Micro-Raman spectroscopy was used to examine molecular structure of the B-NCD films (sp^3/sp^2 band ratio). Optical properties, thickness and roughness in VIS-NIR wavelength range were investigated by means of ex situ spectroscopic ellipsometry (SE).

It is worth noting that such high sensitivity in relation to the detection of refractive index shifts could be used in various biosensors. Optical sensors are based on, inter alia, surface plasmon resonance [28], integrated optics [29] or the use of evanescence field [30].

For this study, was selected melamine (cyanide, 2,4,6-triamino-1,3,5-triazine), which is the amino group-containing compound, which enables easy modification of the diamond electrode's surface. Baskar *et al.* [31,32] described the electrochemical synthesis of poly-melamine and its application to NADH oxidation. Modification of such compound can be extremely effective in the detection of nucleic acids, such as adenine and guanine, and caffeine [3].

2. Experimental

2.1. Chemicals

0.1 mM Melamine in 0.1 M H_2SO_4 solution was prepared by adding 18 MΩ ultrapure water from E-pure Barnstead system. The supporting electrolyte was 0.1 M (pH 7.0) phosphate buffer prepared by mixing NaH_2PO_4 and Na_2HPO_4 with 18 MΩ ultrapure water. The pH of supporting electrolyte was controlled by means of a FB-5 pH-meter (Fisher Science, USA).

2.2. Electrode growth

B-NCD electrodes were deposited on optically-clear polished quartz substrates (20 mm x 20 mm) in an MWPACVD system (SEKI Technotron AX5400S, Japan). The substrates were seeded via spin coating in nanodiamond slurry by spinning 2 times for 60 s each time. The chamber stage was maintained at 475 °C during the deposition process. A special truncated cone-shaped shim was used during the growth of diamond films [19]. Excited plasma was ignited by microwave radiation (2.45 GHz) [33], and the plasma microwave power was 1300 W. The CH_4:H_2 molar ratio of the mixture was kept at 1% of gas volume at 300 sccm of the total flow rate. The base pressure was about 10^{-6} Torr, and the process pressure was kept at 50 Torr. The boron level, expressed as the [B]/[C] ratio in the gas phase, was 5000 ppm. Diborane (B_2H_6) was used as a dopant precursor. The growth time was 3 h, which resulted in the production of nanocrystalline films with a thickness of approx. 260 nm.

2.3. Surface morphology

Scanning Electron Microscope FEI Quanta FEG 250 with 10 kV beam accelerating voltage and SE-ETD detector (secondary electron - Everhart-Thornley detector) working in high vacuum mode (pressure 10^{-4} Pa) was used to observe the surface structure of B-NCD. The morphological studies were performed with optical microscopy using a combination of a 20x objective magnification and numerical aperture 0.4, and the program for data visualization and analysis (Gwyddion, 2.40, Czech Republic).

2.4. Raman spectroscopy

Raman spectroscopy has been performed by using a Kimmon IK3252R-E excitation source operating at 325 nm. Typically, 10 mW excitation power was used. The laser light was focused on the sample using the quartz objective with 15x magnification, which provided the excitation spot size of about 1.5 μm. No degradation of the sample was detected under such excitation conditions. The UV Raman spectra were collected by using one stage of Jobin Yvon Horiba T64000 spectrometer, equipped with a razor edge filters. The spatial mapping resolution of the system was ca. 0.1 μm. The obtained Raman spectra were analyzed by fitting Lorenztian curves from the software package Wolfram Mathematica 11.2

2.5. Spectroscopic ellipsometry

The ellipsometric parameters, Ψ and Δ, and depolarization factor (%Depol) were measured for three angles of incidence (65°, 70°, and 75°) in the photon energy range from 0.3 to 4.2 eV (4100-295 nm) at room temperature (20 °C) by means of a rotating analyzer device (V-VASE, J.A. Woollam Co. Inc., USA) and a FTIR ellipsometer (Sendira, Sentech GmbH, Germany).

2.6. Thin-layer electrochemical cell & electrochemical polymerization

The spectroelectrochemical measurements were carried out in a homemade, thin-layer cell (Fig. 1(b) and 1(c)). The cell design is shown in Fig. 1. The sample holder and the main body are made of plastic. The optical windows are made from optical-quality quartz glass. A Kapton film spacer (Fig. 1) with a diameter of 9 mm, giving an exposed geometric area of 2.5 cm2, creates a thin-layer cavity ~125 μm thick with a volume of 32 μL. The electrical contact is made by pressing a platinum wire to the surface of electrode unexposed to the electrolyte solution. The counter electrode is made of another Pt wire, while Ag/AgCl serves as a reference electrode with the capillary connection to electrolyte.

The cleaning protocol for electrochemical cell was bath in ultrapure isopropanol alcohol and water before each measurements. After a series of measurement was added ultrasonic bath for better cleaning.

Cyclic voltammetry (CV) electropolymerization were carried out in solution of 0.1 M H_2SO_4 consisting 0.1 mM Melamine in scan rate of 0.1 $V \cdot s^{-1}$. The electrochemical experiment was performed by using an Autolab potentiostat/galvanostat (PGSTAT30 and GPES 4.9 software/Nova 1.10.2, Netherlands).

2.7. Mach-Zehnder setup

The measuring system was based on MZI, which has been built on Thorlabs bulk components, including non-polarization beam splitter, silver mirrors, and collimators with a focal length f of 18.07 nm and a numerical aperture NA equal to 0.15. Such components were selected in order to work in the visual range. The tunable laser TLB-6304 (New Focus) has been used as the coherent light source, which provided fine tuning over the wavelength range from 631.05 to 635.05 nm, with a tuning rate of 5 nm/s. The optical interference signal was recorded with a multifunctional optical power meter model 1835-C (Newport) connected to a digital oscilloscope.

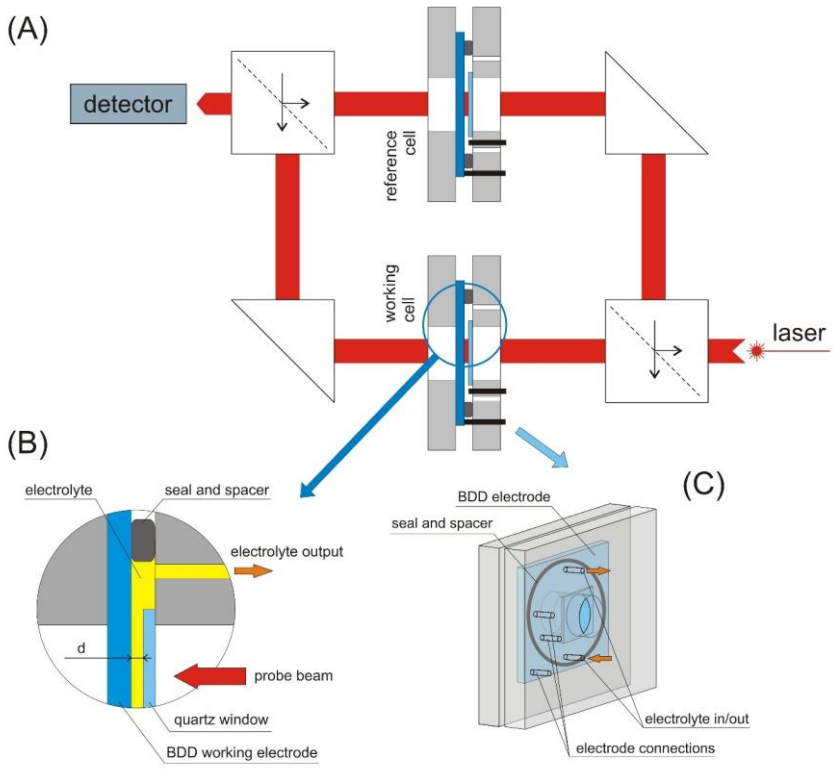

Figure 1. (A) Scheme of Mach-Zehnder interferometer with thin-layer electrochemical cells, (B) construction of a measuring cell, and (C) thin-layer electrochemical cell.

3. Results and discussion

3.1. B-NCD electrode surface morphology and chemical composition analysis

The key factor to achieve high optical transmittance is to produce nanocrystalline diamond films which contain crystallites smaller than 100 nm. The properties of nanocrystalline diamond can be approximated to the monocrystalline diamond [34], which depends on the nucleation density [35], and the surface expansion to volume ratio, and therefore on the content of the sp^2 phase and hydrogen contamination [36]. Fig. 2 shows the crystallite size distribution, where 72% of crystallites is below 60 nm, and 24% are in the range from 60 nm to 100 nm. Furthermore, low surface roughness of ca. 10 nm was achieved without any additional treatment. This finding is crucial for working with optical signals because the optical scattering increases with increasing surface roughness.

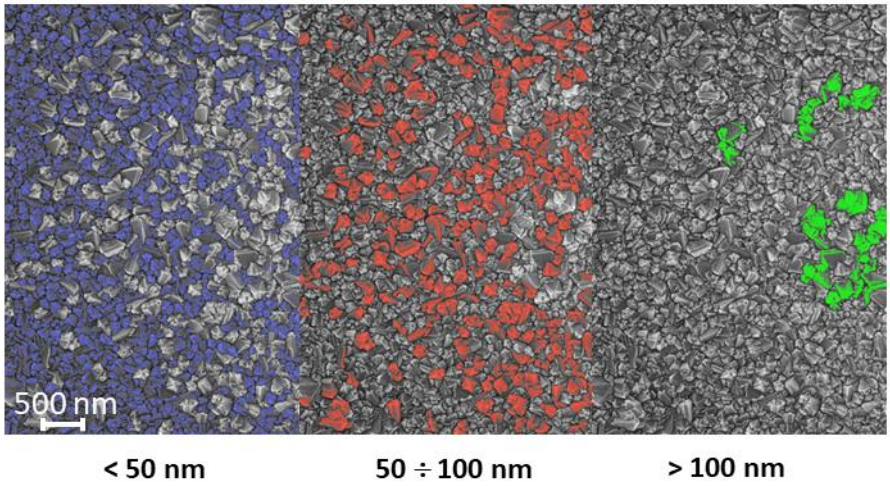

Figure 2. SEM micrograph of B-NCD sample with the marked size distribution of crystallites.

The further analysis of sample homogeneity, as well as its chemical composition analysis, were performed using UV Raman Spectroscopy. The spectrum, as presented in Fig. 3(a), has several features associated with the structure of boron and carbon. No strong fingerprints of other chemical species have been detected. In the measured spectra, several lines can be observed: the line at 490 cm^{-1} attributable to B-C bonds, the lines related to diamond-like sp^3 carbon structures associated with E_g and F_{2g} modes at ca. 1320 and 600 cm^{-1} respectively [37], and lastly, the structures associated with the sp^2-hybridized carbon structures, i.e. D and G lines observed at 1375 and 1580 cm^{-1}, respectively.

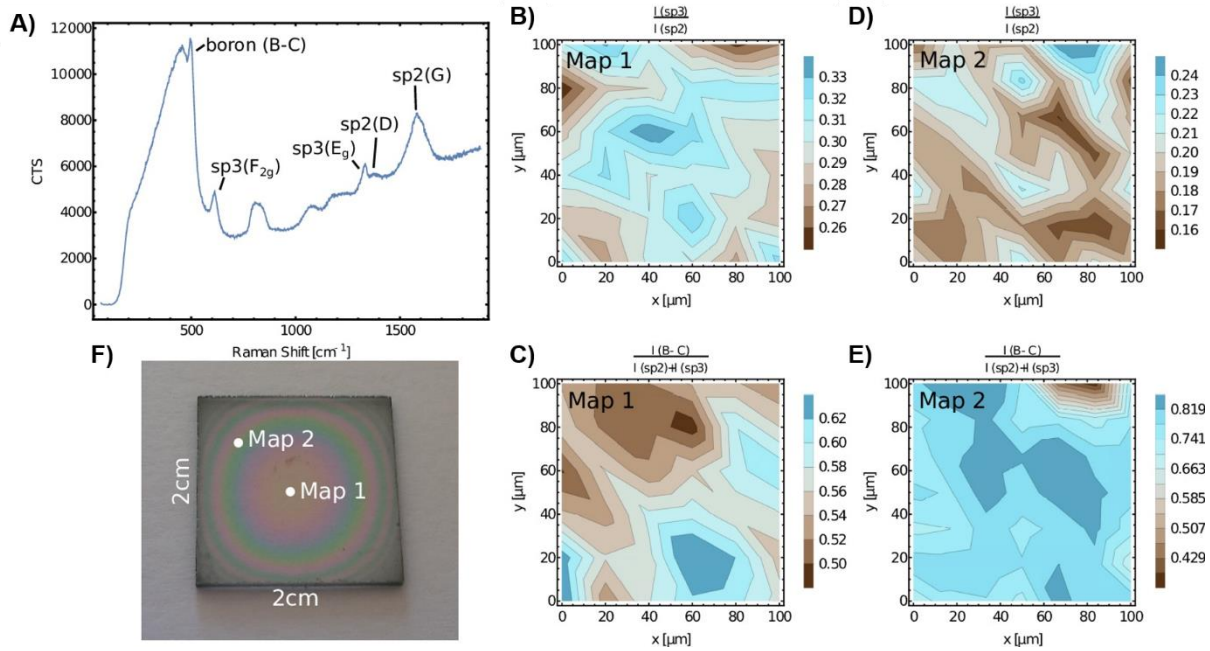

Figure 3. A) Exemplary UV Raman spectrum of B-NCD sample, B, D) maps of intensity ratios of Raman lines associated with the sp^3 and sp^2 hybridization of carbon, recorded at two different points on the sample, C, E) maps of intensity ratios of Raman lines associated with B-C bonds and the sum of sp^2 and sp^3, hybridization of carbon, recorded at two different points on the sample, F) photograph of the sample with mapping sites marked with white dots.

In order to establish the homogeneity of the sample, two 100 μm x 100 μm mapping measurements with the 10 μm step were performed at sites separated by a distance of 10 mm. The maps shown in Fig. 3(b) and 3(d) show a relatively high variation of the intensity ratio of sp^3/sp^2 lines suggesting non-uniform growth of the material at the micron-scale, which is consistent with the SEM analysis. Note that the presented values do not represent ratios of atomic concentrations, and thus should only be compared to each other. Moreover, the variability is also visible on the macro-scale as demonstrated by the mean values of fitting parameters (see Table 1). The standard deviation of the sp^3 intensity values is under 5%, while it becomes higher in the case of sp^2-hybridized carbon structures. This indicates that the sample inhomogeneity visible in the maps is related to the growth of the undesired graphitic-like carbon in the structure, while the variation of the diamond-like material is much more uniform on the micro-scale. At the same time, while the B-C and sp^2 lines do not change their intensity significantly between the two mapped sites, the difference in sp^3 line intensity is significant, suggesting that the diamond layer may have different thickness in those areas. This is also noticeable in the color interference patterns; the phenomenon is clearly visible on the surface of the sample with a naked eye (Fig. 3 (f)).

Table 1. The parameters of fitted curves related to Raman lines associated with B-C bonds, and sp^3 (E_g) and sp^2 hybridization.

######	**Map 1**	**Map 2**
Intensity (B-C)	35000 ± 1300	34000 ± 1800
Position (B-C)	495.9 ± 0.4	496.3 ± 0.2
FWHM (B-C)	26.5 ± 1.0	26.4 ± 0.4
Intensity (sp^3)	14400 ± 1200	7500 ± 1400
Position (sp^3)	1331.1 ± 0.3	1331.8 ± 0.6
FWHM (sp^3)	21.5 ± 1.3	26.3 ± 2.9
Intensity (sp^2)	48000 ± 3000	38000 ± 3500
Position (sp^2)	1582.9 ± 1.0	1584.5 ± 0.7
FWHM (sp^2)	61.7 ± 1.7	65.6 ± 1.0

While the ratio of the signals corresponding to the sp^2- and sp^3-hybridized carbon structures exhibits spatial variation, it is noteworthy that other fitting parameters (peak position, FWHM) remain consistent on the surface of the sample, indicating negligible differences in the mechanical strain or disorder in the sample. This, together with the previously described low variation of the sp^3 line intensity, proves that the grown diamond structures are of high quality across the sample.

The analysis of the intensity of Raman lines associated with B-C bonds (Fig. 3(c), 3(e) and Table 1) shows only slight variation of the boron concentration in the material. This finding confirms that the doping process was effective in the growing carbon material in case of both types of hybridization, i.e. sp^3 and sp^2.

3.2. Optical properties of B-NCD electrode

The optical constants and thickness of the electrode were predicted using a five-medium optical model of sample (ambient / rough layer / diamond film / intermix / SiO_2). The optical response of B-NCD film was estimated by using the sum of Drude and Lorentzian oscillators which, in general, describe IR and UV absorption, respectively [38,39]:

$$(\tilde{n})^2 = \tilde{\varepsilon} = \varepsilon_\infty - \frac{(\hbar\omega_p)^2}{E^2 + i\Gamma E} + \frac{A_0 E_0^2}{E_0^2 - E^2 - i\gamma_0 E}, \quad (1)$$

where: $\tilde{n}$ is the complex refractive index ($\tilde{n}$ =n+iκ, n - the refractive index, κ - the extinction coefficient), and $\tilde{\varepsilon}$ is the complex dielectric function of the layer. In Eq. (1), ε_∞ is the high-frequency dielectric constant, ω_p - the plasma frequency, and Γ - the free-carrier damping. The parameters of Lorentzian oscillator, A_0, E_0 and γ_0 represent its amplitude, position, and broadening, respectively. The refractive index of SiO_2 was taken from a database of optical constants [38]. The intermix and rough layers were described as a Bruggeman effective medium approximation (BEMA) [38,39]. The thickness of intermix film was set at 2 nm.

The thickness of the B-NCD and rough layers was found to be 272±2 nm and 11±1 nm, respectively. The Drude parameters determined in this study equal $\hbar\omega_p$=1.30±0.02 eV and $\hbar\Gamma$=2.55±0.13 eV, which is slightly higher than the corresponding values reported earlier by Sobaszek *et al.* [19] for the thinner B-NCD layer with the same [B]/[C] atomic ratio (5k). Fig. 4 shows the refractive index (n) and extinction coefficient (κ) of the B-NCD layer. The shape of the presented spectrum is directly associated with the optical properties of the investigated film. The increase in κ for long wavelengths is related to absorption caused by free electrons (the presence of boron dopant), while for short wavelengths, to interband transition. The transmittance (T) values (see inset in Fig. 4) for wavelengths between 500 nm and 1000 nm ranged from 50% to 55%. A significant decrease in T values for λ<500 nm is associated with the UV-absorption of the B-NCD film. The oscillations in the transmittance spectrum are characteristic for the interference of light in the thin dielectric layer [39].

A detailed analysis of the influence of boron concentration on the optical spectra of B-NCD films as well as their Drude parameters was presented by Sobaszek *et al*. [19].

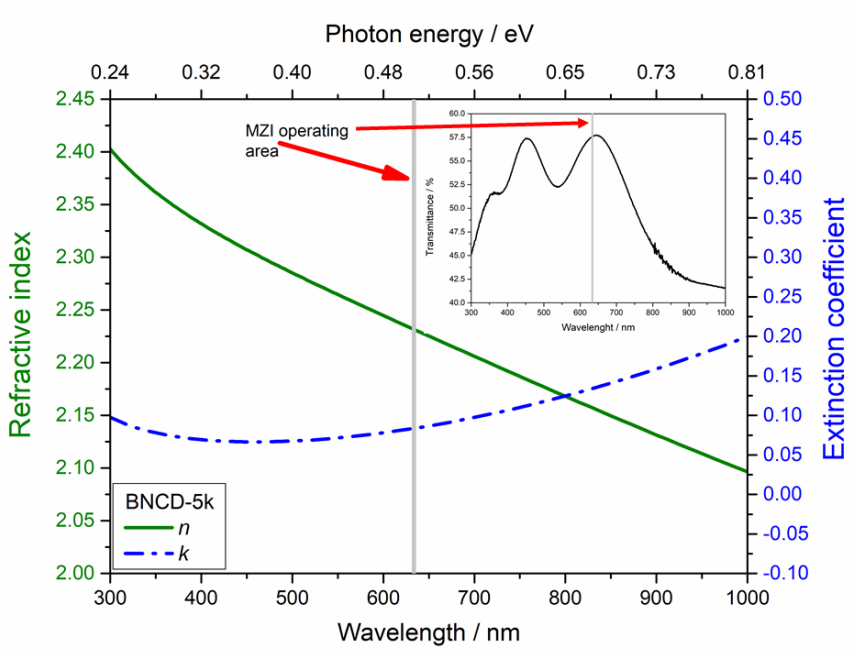

Figure 4. The refractive index and extinction coefficient of the B-NCD film. Inset: the transmittance spectrum of the B-NCD film.

3.3. Evaluation of interferometric-spectroelectrochemical setup

First step of measuring system characterization was electrochemical evaluation of BNCD electrodes. The investigating the electrochemical properties was carried out by cyclic voltammetry which is very useful and easy method. The electrochemical working window is shown on Figure 5A with scan range changing from cathodic -1 V to anodic 1.2 V vs silver/silver chloride reference electrode. In case redox probe system the reversibility of $[Fe(CN)_6]^{3-/4-}$ redox system vs. scan rate is shown on Figure 5B. The value of peak to peak separation for scan rate 50 mV/s is equal to 102 mV which is comparable to GC electrodes. Moreover, which should be noticed the carrier transport is influenced by the grain size and film thickness [40].

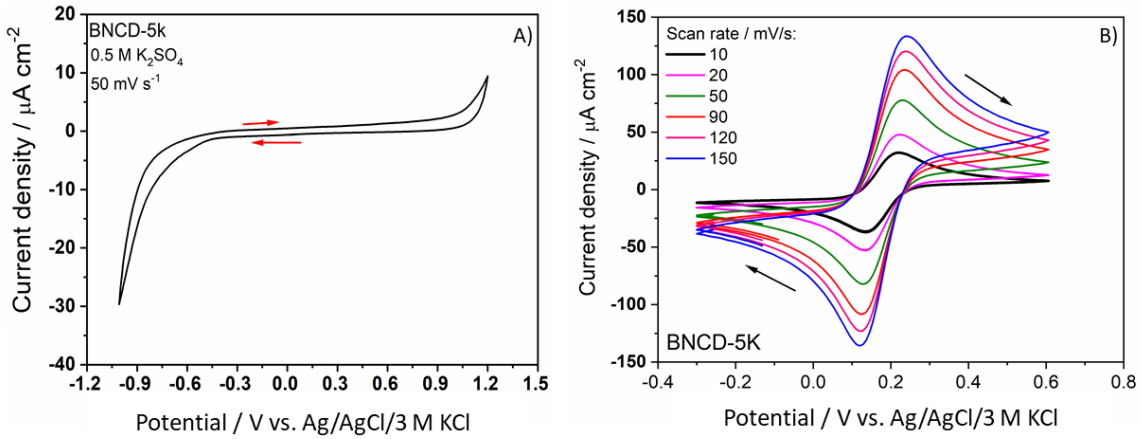

Figure 5. Cyclic voltammograms of the B-NCD electrode in (A) 0.5 M K_2SO_4 solution at scan rate 50 mV/s and (B) K_2SO_4 solution consisting $[Fe(CN)_6]^{3-/4-}$ vs. scan rate.

In any indirect measurements of such quantities like concentration or degree of material degradation wherein the changes of the optical parameters are linked to the measured value, it is necessary to assess the measurement system resistance to external factors like temperature or noise. In the presented case, influence on the measurements might be the result of variables such as mass transport, temperature and stability of laser, which had to be investigated before conducting the experiment. In order to evaluate the optical method and experimental system robustness the series of measurements, taken for high electrical potential, were carried out. Both working and reference cells were filled up with pH 7.2, 0.1 M PBS electrolyte. On the working electrode was applied potential +1 V and -1 V for 10 min. The modulation over the optical light source spectral range has been observed and recorded. Such measurements were carried out every 60 s. The results for positive and negative electrodes polarization have been presented in the Fig. 5. The measure of the measurement system stability is the invariability of the phase between the recorded signals. Based on experimental results (Fig. 6A and 6B) the standard deviations of the phase variation over time are 0.08π and 0.2π for positive and negative voltage polarizations, respectively. They provide the maximum measurement uncertainty about 10% referring to the 2π maximum phase shift. This value is good enough to express the capabilities of this optical method for substances detection.

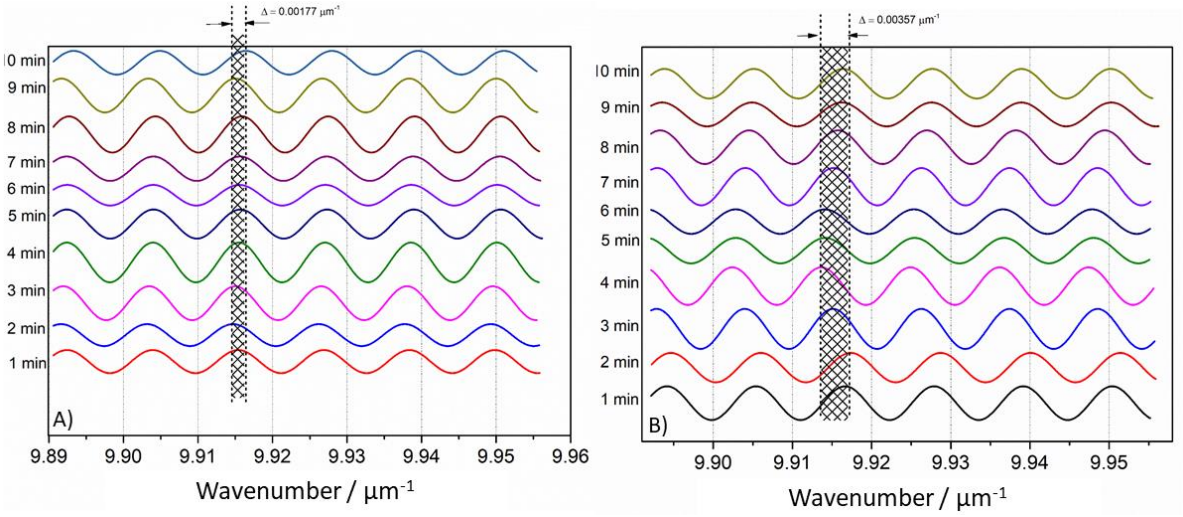

Figure 6. Recorded phase shift for applied potentials A) +1 V and B) -1 V versus Ag/AgCl 3 M KCl reference electrode during 10 minutes.

3.4. In-situ monitoring of boron-doped diamond surface modification

The B-NCD electrode was modified with electro-polymerized melamine by using the procedure described for the BDD electrode modification [3]. Fig. 7A shows the CV voltammograms recorded in potential range from 0 to 1.22 V vs. Ag/AgCl 3M KCl at scan rate 50 mV/s. The inset of Fig. 7A shows the magnification of the anodic peak of melamine at a potential value of 0.62 V. The decreasing current at this oxidation peak for the consecutive scans leads to the formation of polymeric films on the electrode's surface. The poly-melamine polymer forms by a head-to-head reaction with NH-HN groups between the two molecules of melamine.

The process of electro-polymerization has to be carried out in acidic medium, and an increase in the acid concentration reduces the polymerization time. Fig. 6(b) shows the phase shift during the electrochemical modification of B-NCD electrode with melamine. At the beginning, the phase was measured under stationary conditions without the potential applied to working cell. Next, the phase shift was recorded for the maximum anodic peak (E = 0.62 V).

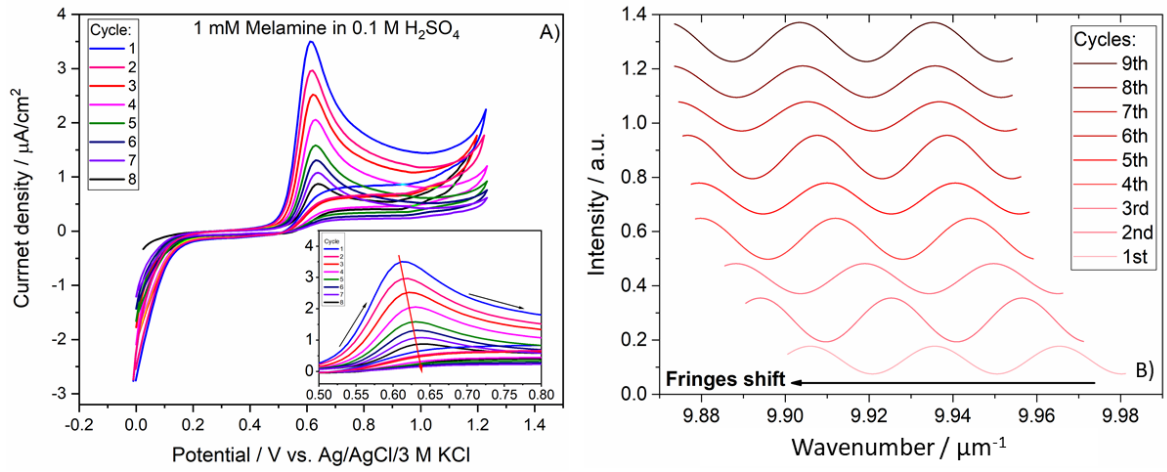

Figure 7. A) Cyclic voltammetry of 1 mM melamine in 0.1 M H_2SO_4 with a scan rate of 50 mV/s; inset: magnification of anodic peak during electropolymerization of melamine, and B) phase shift during electro-polymerization of melamine; steps were recorded at the anodic peak.

The most significant phase shift was observed during the first three CV cycles, reaching 0.01, 0.0169 and 0.02335 µm^{-1}, respectively (see Fig. 7B). This can be explained by the formation of thin poly-melamine film on the electrode's surface and a change in the refractive index of the solution. The maximum recorded phase shift was 0.0328 µm^{-1} for the last cycle, which corresponds to surface coverage by poly-melamine. After the last CV cycle, no modification reaction occurred, which remains in agreement with the eighth cycle on the CV curve (see Fig. 7A) where the current of oxidation peak significantly decreased. Furthermore, after the 4th cycle, the phase shift became less significant what could be attributed to surface blocking for further melamine electropolymerization. This can be explain by surface hinderance to the electron transfer of negatively charged $[Fe(CN)_6]^{3-/4-}$ redox system. The Figure 8 shows CV voltammograms before (black) and after modification process (blue) recorded in 0.5 M K_2SO_4 consisting 5 mM $[Fe(CN)_6]^{3-/4-}$ vs. at scan rate 50 mV/s. Also, the significantly change in peak to peak separation can be seen from 112 mV before to over 700 mV after electro-polymerization (eight cycle). Moreover, the decreasing trend of the recorded oxidation current shows a good correlation with the phase shift (see Fig. 9). The plotted curve of phase shift vs. oxidation peak current displays a similar variability. Kim *et al.* [41] used the phenomenon of interferometry to determine the crystal growth rate.

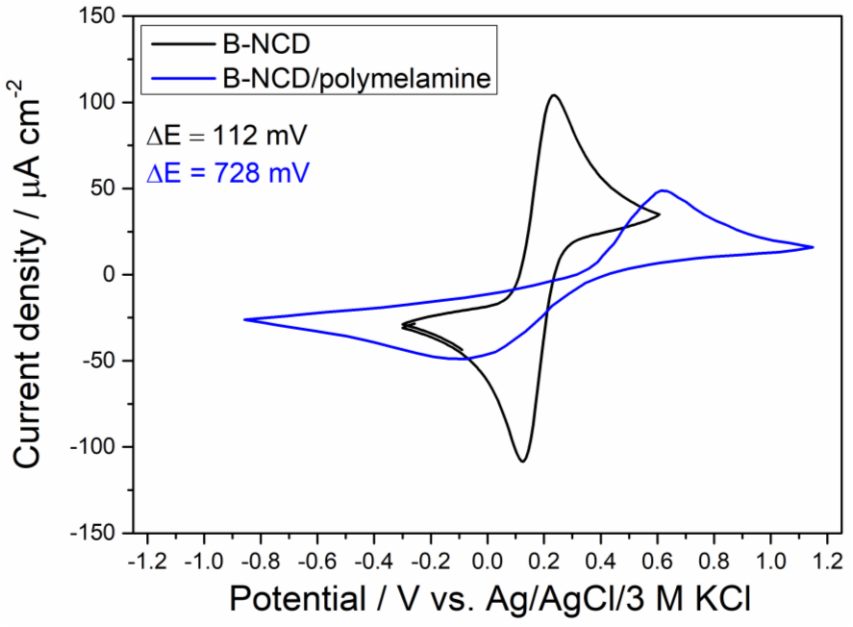

Figure 8. Cyclic voltammograms of the B-NCD electrode before (A) and after electropolymerization of melamine in 0.5 M K_2SO_4 consisting 5 mM $[Fe(CN)_6]^{3-/4-}$ vs. Ag/AgCl/ 3 M KCl reference electrode at scan rate 50 mV/s.

The repeatability studies were conducted during independent electropolymerization processes of melamine at separately deposited B-NCD electrodes. Three freshly prepared electrodes have been used for the monitoring processes. The three replicate phase shift measurements in 1 mM solution of melamine resulted in the avg. RSD value of 1.4 %, while three separately grown electrodes in the same conditions revealed avg. RSD value of 3.6 % in 1 mM solution of melamine.

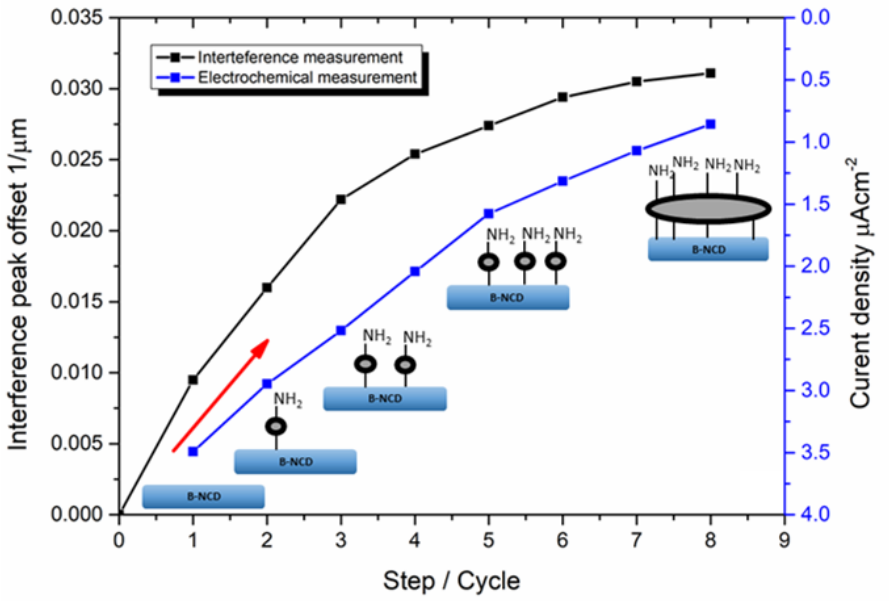

Figure 9. Phase shift versus recorded current during electropolymerization of melamine.

4. Conclusions

The chemical analysis, based on the Raman measurements, confirmed the presence and high purity of boron dopant in the sample. While it has been confirmed that doping is more effective in the graphitic-like carbon that forms during the growth process, it was also proven that doping occurs in the diamond-like carbon as well. The optical transmittance of the B-NCD electrode reached 55% for the wavelength range under the operating are of the measuring system, which allows to combine optical and electrochemical investigations.

The optical interferometry was successfully applied to *in-situ* monitoring of electropolymerization of melamine at B-NCD electrode surface. This technique is a powerful tool for interactions occurring on the surface of the electrode during electrochemical reactions. Achieved results, show that the described setup may be applicable to monitoring of surface modifications by various necessary linkers, like investigated melamine, or others like poly-l-lysine, antibodies, metals and so on. Moreover, the electrochemical result show good correlation with optical measurements, which are promising results for future development of measuring system. Furthermore, the presented method allows for detecting compounds whose products accumulate on the electrode, a process which is considered negative from the electrochemical point of view. The future experiments will focus on the surface modification with linkers, and DNA detection.

Acknowledgment

This work was supported by the National Science Centre (NCN) under Grants No. 2016/21/B/ST7/01430 and 2017/01/X/ST7/02045 and The National Centre for Research and Development Techmatstrateg 347324/12/NCBR/2017. The DS funds of the Faculty of Electronics, Telecommunications and Informatics, and the Faculty of Chemistry at the Gdansk University of Technology are also acknowledged.

References

[1] R. Bogdanowicz, M. Sawczak, P. Niedzialkowski, P. Zieba, B. Finke, J. Ryl, J. Karczewski, T. Ossowski, Novel Functionalization of Boron-Doped Diamond by Microwave Pulsed-Plasma Polymerized Allylamine Film, The Journal of Physical Chemistry C. 118 (2014) 8014–8025. doi:10.1021/jp5003947.

[2] C.E. Nebel, N. Yang, H. Uetsuka, E. Osawa, N. Tokuda, O. Williams, Diamond nano-wires, a new approach towards next generation electrochemical gene sensor platforms, Diamond and Related Materials. 18 (2009) 910–917. doi:10.1016/j.diamond.2008.11.024.

[3] P. Niedziałkowski, R. Bogdanowicz, P. Zięba, J. Wysocka, J. Ryl, M. Sobaszek, T. Ossowski, Melamine-modified Boron-doped Diamond towards Enhanced Detection of Adenine, Guanine and Caffeine, Electroanalysis. 28 (2016) 211–221. doi:10.1002/elan.201500528.

[4] H. Zhuang, V.V.S.S. Srikanth, X. Jiang, I. Aronov, B.W. Wenclawiak, J. Luo, H. Ihmels, Elucidation of Different Steps Involved in Allylamine Functionalization of the Diamond Surface and Its Polymerization by Time-of-Flight Secondary Ion Mass Spectrometry, Chem. Mater. 22 (2010) 4414–4418. doi:10.1021/cm1009674.

[5] S. Szunerits, R. Boukherroub, Different strategies for functionalization of diamond surfaces, J Solid State Electrochem. 12 (2008) 1205–1218. doi:10.1007/s10008-007-0473-3.

[6] T. Tsubota, O. Hirabayashi, S. Ida, S. Nagaoka, M. Nagata, Y. Matsumoto, Chemical modification of hydrogenated diamond surface using benzoyl peroxides, Phys. Chem. Chem. Phys. 4 (2002) 806–811. doi:10.1039/B107349B.

[7] H. Notsu, T. Tatsuma, A. Fujishima, Tyrosinase-modified boron-doped diamond electrodes for the determination of phenol derivatives, Journal of Electroanalytical Chemistry. 523 (2002) 86–92. doi:10.1016/S0022-0728(02)00733-7.

[8] T. Strother, T. Knickerbocker, Russell, J.E. Butler, L.M. Smith, R.J. Hamers, Photochemical Functionalization of Diamond Films, Langmuir. 18 (2002) 968–971. doi:10.1021/la0112561.

[9] H. Notsu, T. Fukazawa, T. Tatsuma, D.A. Tryk, A. Fujishima, Hydroxyl Groups on Boron-Doped Diamond Electrodes and Their Modification with a Silane Coupling Agent, Electrochem. Solid-State Lett. 4 (2001) H1–H3. doi:10.1149/1.1346556.
[10] A.J. Saterlay, J.S. Foord, R.G. Compton, An Ultrasonically Facilitated Boron-Doped Diamond Voltammetric Sensor for Analysis of the Priority Pollutant 4-Chlorophenol, Electroanalysis. 13 (2001) 1065–1070. doi:10.1002/1521-4109(200109)13:13<1065::AID-ELAN1065>3.0.CO;2-5.
[11] V.C. Diculescu, S. Kumbhat, A.M. Oliveira-Brett, Electrochemical behaviour of isatin at a glassy carbon electrode, Analytica Chimica Acta. 575 (2006) 190–197. doi:10.1016/j.aca.2006.05.091.
[12] M.H. Ahmed, J.A. Byrne, J.A.D. McLaughlin, A. Elhissi, W. Ahmed, Comparison between FTIR and XPS characterization of amino acid glycine adsorption onto diamond-like carbon (DLC) and silicon doped DLC, Applied Surface Science. 273 (2013) 507–514. doi:10.1016/j.apsusc.2013.02.070.
[13] S. L. Candelaria, B. B. Garcia, D. Liu, G. Cao, Nitrogen modification of highly porous carbon for improved supercapacitor performance, Journal of Materials Chemistry. 22 (2012) 9884–9889. doi:10.1039/C2JM30923H.
[14] J.K. Zak, J.E. Butler, G.M. Swain, Diamond Optically Transparent Electrodes: Demonstration of Concept with Ferri/Ferrocyanide and Methyl Viologen, Anal. Chem. 73 (2001) 908–914. doi:10.1021/ac001257i.
[15] J. Stotter, S. Haymond, J.K. Zak, Y. Show, Z. Cvackova, G.M. Swain, Optically transparent diamond electrodes for UV-Vis and IR spectroelectrochemistry, Interface. 12 (2003) 33–38.
[16] S. Gupta, A. Dudipala, O.A. Williams, K. Haenen, E. Bohannan, Ex situ variable angle spectroscopic ellipsometry studies on chemical vapor deposited boron-doped diamond films: Layered structure and modeling aspects, Journal of Applied Physics. 104 (2008) 073514. doi:10.1063/1.2990058.
[17] S. Gupta, B.R. Weiner, G. Morell, Spectroscopic ellipsometry studies of nanocrystalline carbon thin films deposited by HFCVD, Diamond and Related Materials. 10 (2001) 1968–1972. doi:10.1016/S0925-9635(01)00387-9.
[18] W. Gajewski, P. Achatz, O.A. Williams, K. Haenen, E. Bustarret, M. Stutzmann, J.A. Garrido, Electronic and optical properties of boron-doped nanocrystalline diamond films, Phys. Rev. B. 79 (2009) 045206. doi:10.1103/PhysRevB.79.045206.
[19] M. Sobaszek, Ł. Skowroński, R. Bogdanowicz, K. Siuzdak, A. Cirocka, P. Zięba, M. Gnyba, M. Naparty, Ł. Gołuński, P. Płotka, Optical and electrical properties of ultrathin transparent nanocrystalline boron-doped diamond electrodes, Optical Materials. 42 (2015) 24–34. doi:10.1016/j.optmat.2014.12.014.
[20] A. Malinauskas, R. Holze, An in situ spectroelectrochemical study of redox reactions at polyaniline-modified ITO electrodes, Electrochimica Acta. 43 (1998) 2563–2575. doi:10.1016/S0013-4686(97)10176-1.
[21] D.L. Jeanmaire, R.P. Van Duyne, Surface raman spectroelectrochemistry: Part I. Heterocyclic, aromatic, and aliphatic amines adsorbed on the anodized silver electrode, Journal of Electroanalytical Chemistry and Interfacial Electrochemistry. 84 (1977) 1–20. doi:10.1016/S0022-0728(77)80224-6.
[22] A.A. Popov, N. Chen, J.R. Pinzón, S. Stevenson, L.A. Echegoyen, L. Dunsch, Redox-Active Scandium Oxide Cluster inside a Fullerene Cage: Spectroscopic, Voltammetric, Electron Spin Resonance Spectroelectrochemical, and Extended Density Functional Theory Study of Sc4O2@C80 and Its Ion Radicals, J. Am. Chem. Soc. 134 (2012) 19607–19618. doi:10.1021/ja306728p.
[23] T. Allsop, R. Reeves, D.J. Webb, I. Bennion, R. Neal, A high sensitivity refractometer based upon a long period grating Mach–Zehnder interferometer, Review of Scientific Instruments. 73 (2002) 1702–1705. doi:10.1063/1.1459093.
[24] P. Lu, L. Men, K. Sooley, Q. Chen, Tapered fiber Mach–Zehnder interferometer for simultaneous measurement of refractive index and temperature, Applied Physics Letters. 94 (2009) 131110. doi:10.1063/1.3115029.
[25] Z. Tian, S.S.-H. Yam, J. Barnes, W. Bock, P. Greig, J.M. Fraser, H. Loock, R.D. Oleschuk, Refractive Index Sensing With Mach #x2013;Zehnder Interferometer Based on Concatenating Two Single-Mode Fiber Tapers, IEEE Photonics Technology Letters. 20 (2008) 626–628. doi:10.1109/LPT.2008.919507.
[26] J. Wo, G. Wang, Y. Cui, Q. Sun, R. Liang, P.P. Shum, D. Liu, Refractive index sensor using microfiber-based Mach–Zehnder interferometer, Optics Letters. 37 (2012) 67. doi:10.1364/OL.37.000067.
[27] M. Sobaszek, K. Siuzdak, Ł. Skowroński, R. Bogdanowicz, J. Pluciński, Optically transparent boron-doped nanocrystalline diamond films for spectroelectrochemical measurements on different substrates, IOP Conf. Ser.: Mater. Sci. Eng. 104 (2016) 012024. doi:10.1088/1757-899X/104/1/012024.
[28] S.Y. Wu, H.P. Ho, W.C. Law, C. Lin, S.K. Kong, Highly sensitive differential phase-sensitive surface plasmon resonance biosensor based on the Mach–Zehnder configuration, Optics Letters. 29 (2004) 2378. doi:10.1364/OL.29.002378.
[29] B.J. Luff, J.S. Wilkinson, J. Piehler, U. Hollenbach, J. Ingenhoff, N. Fabricius, Integrated Optical Mach-Zehnder Biosensor, J. Lightwave Technol., JLT. 16 (1998) 583.

[30] R.G. Heideman, R.P.H. Kooyman, J. Greve, Performance of a highly sensitive optical waveguide Mach-Zehnder interferometer immunosensor, Sensors and Actuators B: Chemical. 10 (1993) 209–217. doi:10.1016/0925-4005(93)87008-D.
[31] S. Baskar, C.-W. Liao, J.-L. Chang, J.-M. Zen, Electrochemical synthesis of electroactive poly(melamine) with mechanistic explanation and its applicability to functionalize carbon surface to prepare nanotube–nanoparticles hybrid, Electrochimica Acta. 88 (2013) 1–5. doi:10.1016/j.electacta.2012.10.040.
[32] S. Baskar, N. Thiyagarajan, J.-L. Chang, J.-M. Zen, Exploring Redox Behavior of Neutral pH Active Poly(melamine) and Its Electrocatalytic Origination towards NADH Detection, Electroanalysis. (2015) n/a-n/a. doi:10.1002/elan.201500280.
[33] R. Bogdanowicz, M. Sobaszek, J. Ryl, M. Gnyba, M. Ficek, Ł. Gołuński, W.J. Bock, M. Śmietana, K. Darowicki, Improved surface coverage of an optical fibre with nanocrystalline diamond by the application of dip-coating seeding, Diamond and Related Materials. 55 (2015) 52–63. doi:10.1016/j.diamond.2015.03.007.
[34] O.A. Williams, A. Kriele, J. Hees, M. Wolfer, W. Müller-Sebert, C.E. Nebel, High Young's modulus in ultra thin nanocrystalline diamond, Chemical Physics Letters. 495 (2010) 84–89. doi:10.1016/j.cplett.2010.06.054.
[35] J. Philip, P. Hess, T. Feygelson, J.E. Butler, S. Chattopadhyay, K.H. Chen, L.C. Chen, Elastic, mechanical, and thermal properties of nanocrystalline diamond films, Journal of Applied Physics. 93 (2003) 2164–2171. doi:10.1063/1.1537465.
[36] S. Michaelson, O. Ternyak, A. Hoffman, O.A. Williams, D.M. Gruen, Hydrogen bonding at grain surfaces and boundaries of nanodiamond films detected by high resolution electron energy loss spectroscopy, Applied Physics Letters. 91 (2007) 103104. doi:10.1063/1.2779848.
[37] V.D. Blank, V.N. Denisov, A.N. Kirichenko, M.S. Kuznetsov, B.N. Mavrin, S.A. Nosukhin, S.A. Terentiev, Raman scattering by defect-induced excitations in boron-doped diamond single crystals, Diamond and Related Materials. 17 (2008) 1840–1843. doi:10.1016/j.diamond.2008.07.004.
[38] J.A. Woollam, Guide to Using WVASE32®, Wextech Systems Inc., 310 Madison Avenue, Suite 905, New York, NY 10017, 2010.
[39] H. Fujiwara, Spectroscopic Ellipsometry: Principles and Applications, Wiley-Blackwell, Chichester, England ; Hoboken, NJ, 2007.
[40] M. Nesládek, D. Tromson, C. Mer, P. Bergonzo, P. Hubik, J.J. Mares, Superconductive B-doped nanocrystalline diamond thin films: Electrical transport and Raman spectra, Appl. Phys. Lett. 88 (2006) 232111. doi:10.1063/1.2211055.
[41] Y.-K. Kim, B.R. Reddy, T.G. George, R.B. Lal, Optical heterodyne interferometry technique for solution crystal growth rate measurement, Optical Engineering. 37 (1998) 616–622.

Biographies

Michał Sobaszek was born in Gdansk in 1984. In the summer of 2009 he received a Master degree in Materials Engineering at Gdansk University of Technology. Currently he is an Assistant Professor at the Faculty of Electronics at Gdansk University of Technology. For more than 5 years, he has gained experience in depositing and characterizing thin films using PA CVD and CVD methods such as diamond semiconductor, nanotube, nanoscale, etc. The main topics of interest are: diamond base, optical and electronic sensors, environmental protection, storage and energy conversion.

Marcin Strąkowski (born 1978) received his Ph.D. degree with honors in Electronics from the Gdansk University of Technology in 2010. Since then he has been an assistant professor in the Department of Metrology and Optoelectronics. His current domains of interest include optoelectronics, optical coherence tomography, low-coherence interferometry, optical sensors and sensing techniques, as well as high power lasers for material processing.

Łukasz Skowroński (born 1982) received his Ph.D. degree in Physics from the Poznań University of Technology in 2013. Currently, he is an assistant professor in the Institute of Mathematics and Physics at UTP University of Science and Technology in Bydgoszcz. His current domains of interest include thin metalic and dielectric films (especially TiO2- based decorative coatings).

Katarzyna Siuzdak (born 1984) received a PhD (2012) and DSc (2017) degrees in chemical technology at Gdańsk University of Technology. In 2011 she spend 3 months in Organic Electronic Group at Bordeaux University of Technology. Since 2012, she is working in Centre of Plasma and Laser Engineering in The Szewalski Institute of Fluid Flow Machinery Polish Academy of Sciences in Gdańsk where she leads The Laboratory of Functional Materials. In 2016 she received START scholarship from the Foundation for Polish Science and in 2018 - the scholarship for the outstanding young scientists. Her current research is focused on the fabrication and modification of organized titania nanostructures, characterization of photoelectrochemical activity and the ultrasensitive detection of important biologic molecules via non-invasive way.

Mirosław Sawczak (born 1972) is an assistant professor in Centre for Plasma and Laser Engineering of IFFM Polish Academy of Sciences in Gdańsk. In 2003 he defended his doctoral thesis devoted to the diagnosis and shaping parameters of high power technological CO_2 lasers. Since then, he has been dealing with issues related to non-destructive materials testing using laser spectroscopy as well as X-ray fluorescence techniques. He has extensive experience in the design and construction of laser based and X-ray research equipment. For many years he conducted research on the application of non-destructive analytical techniques in the study of historical objects as well as application of lasers in cultural heritage conservation. More recent research is devoted to spintronics, nanomaterials and functional materials in application for sensors.

Igor Wlasny (born 1985) received his PhD degree with honors in Physics in 2014 A.D. on University of Lodz in Poland. Working in Lodz he worked on investigating the phenomenon of corrosion in graphene-coated copper and developing the technology of graphene-based inkjet printing. In 2015 he has moved to Institute of Experimental Physics in University of Warsaw, where he currently works on a post-doc position. His current research interests involve the interactions within 2D heterostructures.

Andrzej Wysmołek is a professor at the Faculty of Physics, University of Warsaw. He worked at the Max Planck Institute, Stuttgart (one year) as Alexander von Humboldt postdoctoral fellow, and at the Centre National de la Recherche Scientifique, High Magnetic Field Laboratory, Grenoble, France (18 months). He is an expert in the optical spectroscopy of solid state systems: bulk semiconductors, semiconductor nanostructures, graphene, graphene oxide and other 2D materials like transition metal dichalcogenides. He received several awards for his achievements in science and science popularization including the Award of the Capital City of Warsaw (2014) for the popularization of physics.

Aleksandra Wieloszyńska (born 1993) graduated 1st and 2nd degree studies in Electronics and Telecommunications at the Department of Electronics, Telecommunications and Informatics of Gdańsk

University of Technology. Since 2017 she continues studies as a PhD student in the field of Electronics. At the center of her interest are issues related to optics and interferometry. For few years she has involved in the SPIE&OSA Student Chapters activities.

Jerzy Pluciński received the M.Sc. degree in electronics at the Faculty of Electronics, the Gdańsk University of Technology, Poland in 1984, and then in 1994, obtained his Ph.D. degree in optoelectronics (summa cum laude). In 2010, he obtained Habilitated Doctor degree (summa cum laude) at the same university. In years 1991 and 1992, he took two one-month internships at the Universität Karlsruhe, Germany, in 1993 – an one-month internship at the Université de Strasbourg, France, and in 1996 – a six-month postdoc internship at the Measurement and Sensor Laboratory in Kajaani, University of Oulu, Finland. In years from 1997 to 2003, he worked for 21 months at the Optoelectronics and Measurement Techniques Laboratory, the University of Oulu, Finland. He has research interests in optoelectronics and photonics, optics of highly scattering materials, optical coherence tomography, low-coherence interferometry, optical fiber sensors, and laser technics. He is the author or co-author of over 150 scientific papers, the author of 1 monography, 1 academic handbook, and 2 chapters in 2 international academic handbooks. Now he is Professor at the Gdańsk University of Technology. He directs there the Optoelectronics Team at the Department of Metrology and Optoelectronics at the Faculty of Electronics, Telecommunications and Informatics.

Robert Bogdanowicz (born 1976) received his Ph.D. degree with honours in Electronics from the Gdansk University of Technology in 2009. He worked as a post-doc researcher in Ernst-Moritz-Arndt-Universität Greifswald Institut für Physik in 2010 and 2011. He has initiated optical emission imaging of muti-magnetron pulsed plasma and contributed to the development of antibacterial implant coatings deposited by high-power impulse magnetron sputtering. He moved back to the Gdansk University of Technology in 2011, as an assistant professor in the Department of Metrology and Optoelectronics. His current domains of interest include selective CVD diamond growth and nanocrystalline diamond doping for environmental and biochemical nanosensors. He is the head of research group and member of the board operating within Advanced Technologies Centre "Pomerania", created in the framework of the Operational Programme for the development of innovative companies. Certified manager IPMA (D) and took part in the first edition of the Top 500 Innovators (Stanford University). In 2011-2015, he was the manager of programs LEADER NCBiR and Sonata NCN. In 2015 he held a scholarship Fulbright Senior Scholar Program at the California Institute of Technology (Caltech) in the group of prof. William Goddard (Materials and Process Simulation Center) working on hybrid 3D diamond structures.